Optically Triggered Chaotic Vortex Avalanches in Superconducting $YBa_2Cu_3O_{7-x}$ Films

You-He Zhou,[1,2,*] Cunhong Wang,[1,2] Cong Liu,[1,2] Huadong Yong,[1,2] and Xingyi Zhang[1,2,†]

[1] *Key Laboratory of Mechanics on Disaster and Environment in Western China attached to the Ministry of Education of China, Lanzhou University, Lanzhou, Gansu 730000, People's Republic of China*

[2] *Department of Mechanics and Engineering Sciences, College of Civil Engineering and Mechanics, Lanzhou University, Lanzhou, Gansu 730000, People's Republic of China*

(Received 28 November 2019; revised manuscript received 7 January 2020; accepted 15 January 2020; published 13 February 2020)

Flux avalanche is commonly found in type II superconductors, and this event is always featured as being unpredictable and having ultrafast development with time. It is difficult to capture dynamically by any experimental method available today. Here, we propose a hypervelocity magnetic-optical system with two optical branches; one branch can trigger a dendritic flux avalanche in a superconducting film, and the other is capable of producing continuous multiexposure to record the lightning avalanche process. In contrast with some traditional trigger models, the present method realizes control of the position where the flux avalanche takes place. Second, we study the sensitive dependence on initial conditions of the present flux avalanche and find a series of positive Lyapunov exponents between two adjacent trajectories, which can be considered direct evidence for the chaotic dynamics in this kind of avalanche. Moreover, we reveal that, whether the laser spot is in the Meissner state or the mixed state, avalanches always penetrate from the edge of the superconducting film to the Meissner region, instead of occurring around the laser spot. This behavior clearly demonstrates that the presented avalanche is driven by the magnetic pressure force, which suggests that the optically triggered vortex avalanche possesses a different mechanism from that of the thermomagnetic avalanches commonly found in superconducting films.

DOI: 10.1103/PhysRevApplied.13.024036

I. INTRODUCTION

The stability of vortices is critically important for applications of type II superconductors. Dendritic flux avalanche, one of representative modes of flux motion, is observed by magnetic-optical imaging (MOI) in films of many superconducting materials, such as Nb [1,2], NbN [3–5], MgB_2 [6–8], and $YBa_2Cu_3O_{7-x}$ [9–14]. In these experimental processes, magnetic-field sweep, which is the application of current or voltage, is often used to trigger the dendritic flux avalanche. In 1993, Leiderer *et al.* [14] presented a new flux avalanche process triggered by a pulse laser and gave an approximate penetration speed of 50 km/s. In 2003, an avalanche speed of over 180 km/s [15] was found in $YBa_2Cu_3O_{7-x}$ thin films by using a disconnected double-exposure technology. Recently, a trigger method using microwaves was proposed [16–18]. Moreover, numerical simulations [19–23] coupled to the equation describing the production and transfer of heat have been performed to solve the nonlinear and nonlocal electrodynamics of type II superconducting films (or thin disks). These simulations provide an efficient framework for understanding the dynamic properties of dendritic flux avalanches. From the above experimental and simulated results, it is found that research into the vortex avalanche is still faced with the characteristics of being irreproducible, and it is difficult to control the avalanche process.

The mechanism of flux avalanche is a longstanding topic that is still of considerable current interest [24]. It is widely accepted that flux avalanches often originate from a thermomagnetic instability (thermally driven). A dynamically driven mechanism has been proposed for vortex avalanches triggered by a slow drive (a gentle magnetic field) [25], similar to sandpile avalanches, where the interactions among vortices are expected to control the dynamics. In 2012, Qviller *et al.* [26] studied the quasi-one-dimensional (quasi-1D) intermittent flux penetration of $YBa_2Cu_3O_{7-x}$ films on inclined substrates, and they found that the quasi-1D flux avalanche exhibited self-organized criticality (SOC), but did not belong to the series of films commonly exhibiting thermomagnetic instability. It is still a challenge to control and reveal the physical mechanism of the avalanche process at present.

*zhouyh@lzu.edu.cn
†zhangxingyi@lzu.edu.cn

One of the fascinating features of a nonlinear system is that it can exhibit sensitive dependence on initial conditions (SDIC), which is a property of classically chaotic systems [27,28]. Quantized fluxes created via the formation of vortices [29] in type II superconductors can be considered one of feasible ways to investigate quantum chaos [30]. Studies often use an overdamped Langevin dynamics equation to simulate vortex motion. Olive and Soret [31] simulated the chaotic dynamics of superconductor vortices in the plastic phase and presented positive Lyapunov exponents. Lu-Dac and Kabanov [32] considered flux penetration into a two-dimensional superconducting cylinder and found that, when the external magnetic field was over the field limit, the flux penetration became stochastic. Moreover, charge-density waves and Josephson junction arrays have been analyzed through chaos theory [33–37], but there has been no such experimental study for flux avalanches.

Here, we use a pulse laser to trigger a flux avalanche and propose a high-speed MOI with continuous multiexposure to capture evolution of the avalanche over time. By using this technology, we not only find a new chaotic property of flux avalanches, but also present an alternative physical mechanism of the optically triggered avalanche conveniently.

II. EXPERIMENTAL DETAILS

Our $YBa_2Cu_3O_{7-x}$ films (6×6 mm^2) are epitaxial c-oriented films with a thickness of 330 nm deposited on a 10×10 mm^2 lanthanum aluminum oxide ($LaA1O_3$) substrate by magnetron sputtering. The fabrication process is described in Sec. A within the Supplemental Material [38]. The samples are subjected to general zero-field cooling (ZFC), and the measurements are performed in a homemade flow visualization Dewar, which is directly cooled by a commercial GM cryocooler (CSIC PRIDE (Nanjing) Cryogenic Technology Co., Ltd., Model KDE415, 4.2 K@1.5 W). The direction of the magnetic field is perpendicular to the sample plane. To capture the dendritic flux avalanche over time, we use a picosecond laser $\lambda =$ 523 nm, pulse width 600 ps, energy up to 500 μJ at 400 Hz) as a light source to construct the experimental optical system. The avalanche trajectories over time are recorded by multiexposure technology. A sketch of the optical path is displayed in Fig. 1. The laser beam passes through a beam splitter and is divided into two parts: one part triggers the flux avalanche and the other passes through the multiexposure system to record the flux avalanche over time. The exposure time interval is variable. Using our optical system, we can obtain a time difference of double exposure limit of 616.67 ps. If the displacement is assumed to be the full field of the camera, this is equal to 7.0656 mm in this article. So, the maximum speed we can measure is up to the order of 10^7 m/s.

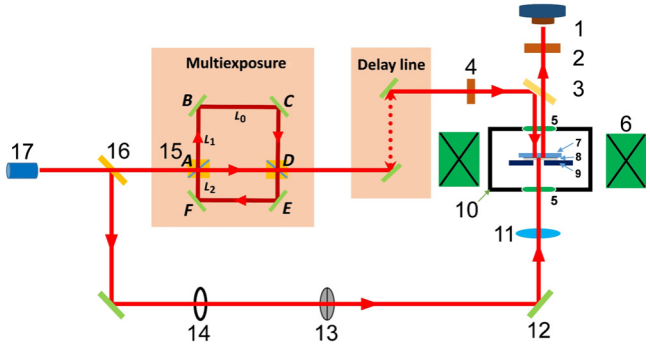

FIG. 1. Schematic of the present experimental setup. 1, CCD camera; 2, analyzer; 3, beam splitter (5:5); 4, polarizer; 5, K9 glass; 6, coil magnet; 7, MO indicator film; 8, sample; 9, cold-end; 10, vacuum cavity; 11, lens; 12, plane mirror; 13, optical modulator; 14, diaphragm, 15, beam-splitter prism (5:5); 16, beam splitter (1:9); 17, picosecond pulse laser (532 nm, 600 ps).

III. RESULTS

Here, we design four exposures to ensure the quality of the MOI figure. When a pulse laser is emitted from the light source, it passes through a beam splitter with an energy division of 1/9; 10% of the laser energy is used to trigger the avalanche and the other 90% enters the exposure path. As displayed in Fig. 1, we have $AD = BC = EF = L_0$, $AB = CD = L_1$, $AF = DE = L_2$, $L_1 = L_2 + L_0$, and $L_2 = 10$ cm. The delay line is used to control the time at which light first reaches the sample surface. If the delay is invariable, the first exposure is achieved at 4.83 ns by the optical path of AD. The second exposure is the superposition of the optical paths $ABCD$ and $ADEFAD$. These paths have the same optical displacement of $2L_1 + L_0$. The aim of this design is to enhance the image quality. The length of L_0 can be chosen to achieve different exposure intervals. In the present experiment, the times of the second, third, and fourth exposures are selected to be 8.77, 12.7, and 16.63 ns, respectively. The avalanche result with superposition of four exposure times is displayed in Fig. 2(a). It should be noted that the fringe superposed on the MO image is caused by interference due to not strictly crossing between the analyzer and polarizer; details can be found in Fig. S1 (Sec. B) within the Supplemental Material [38]. From the side view of the dendritic avalanche, along with the 3D mesh of the gray image shown in Fig. 2(b), by assuming that the gray value is nearly the same within the same exposure time interval, thus, three clear steps are estimated. It should be noted that the final step is the superposition of the third and fourth exposure times because they are indistinguishable. Then the corresponding position coordinates are extracted; the spatial position error is the size of a pixel (7.462 μm). Figure 2(c) displays the magnified gray pattern of the avalanche with four exposure times, in which two tracks are marked as "1" and "2". Selecting track 1

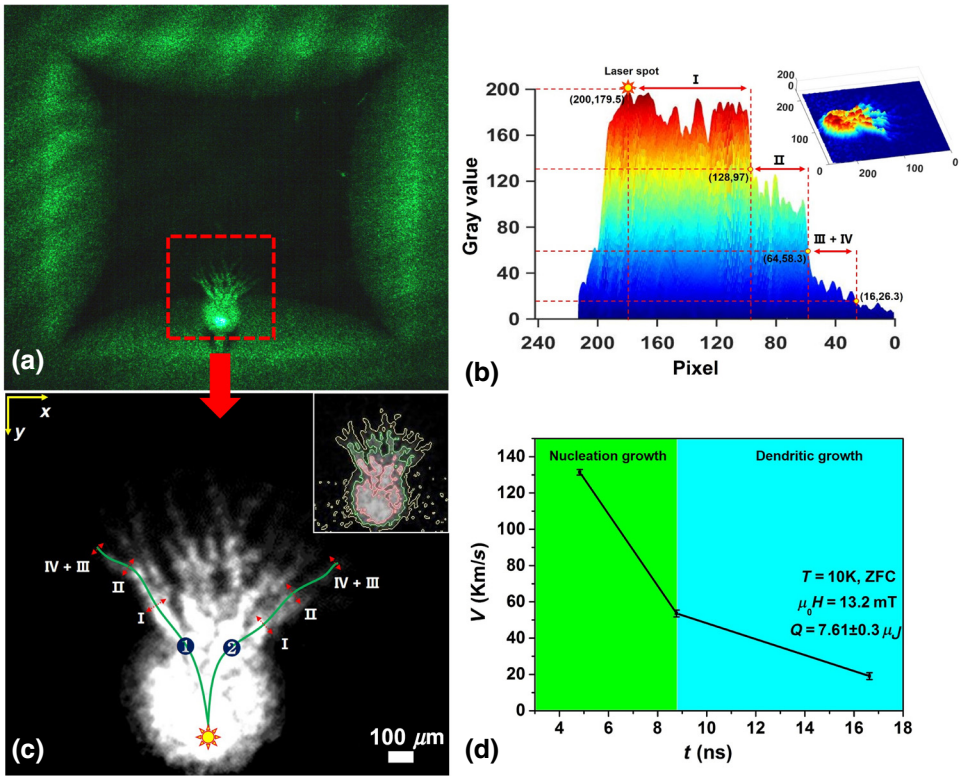

FIG. 2. (a) MO image of avalanches with four exposure times. (b) Side view of gray level of avalanche; three-dimensional (3D) mesh of gray image containing four exposure times as the inset. (c) Grayscale image with edge extraction as the inset. The sun symbol represents the position of the laser point; three dotted red arrows depict edges of the avalanche of four exposure times and are marked I, II, III, and IV. (d) Time-dependent velocity of avalanche at 10 K, ZFC of 13.2 mT, with laser energy of $(7.61 \pm 0.3)\ \mu$J.

to analyze, the time dependence of velocity is displayed in Fig. 2(d); this continuous speed evolution is first obtained and consistent with the simulated results presented by Vestgarden *et al.* [20]. It should be noted that the optically triggered vortex avalanche presented here does not damage the superconducting material. We take the MOI patterns before and after the flux avalanche (the magnetic field and temperature are 25.8 mT and 10 K, respectively) as an example; there is no difference between the two figures, as shown in Fig. 3, which means the superconducting material is not damaged during the experimental process.

We now study the SDIC of the flux avalanches. We present examples in Figs. 4(a)–4(c) of three flux avalanche patterns in a fixed $YBa_2Cu_3O_{7-x}$ sample under the same experimental conditions, where the temperature is 10 K, the magnetic field is 14.7 mT, and the laser energy is $(8.6 \pm 0.2)\ \mu$J. The most important experimental condition is the fixed position of the laser spot. Figure 4(d) displays the superposition of three monochrome color-coded (green, blue, and red) differential images of the dendritic flux avalanches shown in Figs. 4(a)–4(c). No overlapping dendritic trajectories are observed, which implies that the present laser-triggered avalanches are also irreproducible. The energy of each pulse laser is different, and there is a small difference in the output energy, as shown in Fig. S2 within the Supplemental Material [38]. All experimental conditions compose the investigated elements of the SDIC of a nonlinear system. We want to give more direct evidence of SDIC. In general, a positive Lyapunov exponent can be considered a signature of chaotic dynamics in classical and quantum chaos [39–41]. Because of the advantage of the multiexposure technique, the MO image with multiexposure times contains both position and velocity information of the flux front. Therefore, we can construct a phase track in a phase map to describe the flux front behavior. The Lyapunov exponent is used to quantitatively calculate how much the phase track deviates from the balance point. If the

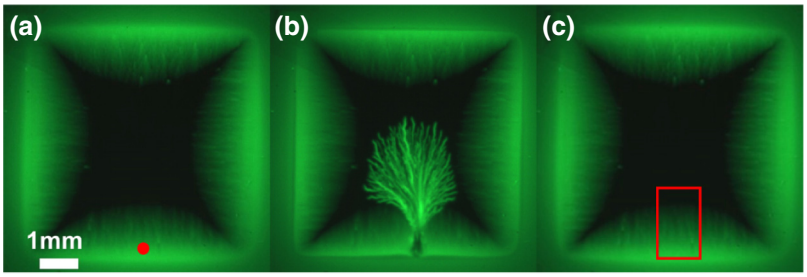

FIG. 3. MO images in ZFC of 10 K, magnetic field of 25.8 mT. (a) The laser point position before the avalanche. (b) Avalanche image captured with laser energy $(4.45 \pm 0.3)\ \mu$J. (c) Sample warmed up above T_c after the avalanche and then subjected to ZFC to the same condition.

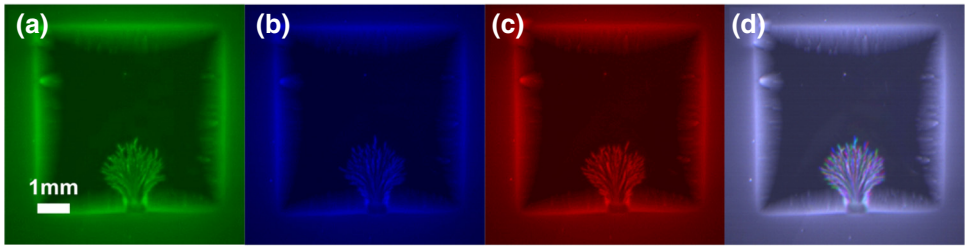

FIG. 4. (a)–(c) Three flux avalanche patterns in a fixed $YBa_2Cu_3O_{7-x}$ sample with the same experimental conditions, where the temperature is 10 K, the magnetic field is 14.7 mT, and the laser energy is $8.6 \pm 0.2\,\mu$J. (d) Superposition of three monochrome color-coded (green, blue, and red) differential images of the dendritic flux avalanches shown in (a)–(c).

Lyapunov exponent is larger than zero, this indicates that the phase track is not stable and chaos happens. The Lyapunov exponent used here has the simplified formula $\lambda = (1/n)\ln(|\delta x_n|/|\delta x_0|) = (1/n)\ln|f^n(x_0)|$, where $|\delta x_n|$ and $|\delta x_0|$ denote the distance in phase space after n iterations and the initial distance between the two trajectories at the same time, respectively. According to our present multiexposure technology, we obtain MOI patterns at the same time to illustrate SDIC. In Figs. 5(a) and 5(b), we present examples of double-exposure flux avalanche grayscale images under the same experimental conditions. Figure 5(c) shows a superposition of the two colors (red and blue), where we can clearly find a trajectory difference with the same exposure time of 8.37 ns. From image processing, we extract five groups of position coordinates, as displayed in the inset of Fig. 5(c), which are substituted into the formula for the Lyapunov exponent. We obtain Lyapunov exponents of $\lambda = 0.034 \pm 0.0087$, 0.035 ± 0.0065, 0.025 ± 0.0061, 0.05 ± 0.0082, and 0.05 ± 0.0082, respectively; these values are all positive. Through the Lyapunov exponent being greater than zero, we prove that the avalanche process shows a chaotic phenomenon, which further demonstrates that the vortex avalanche process is a nonlinear motion system and flux propagation of the avalanche is also random and uncontrollable. Details of the calculation process are given in Sec. C within the Supplemental Material [38]. Therefore, this result can be considered as direct evidence of the chaotic dynamics of the flux avalanche presented in this article.

We now discuss the physical mechanism of the present flux avalanche triggered by a pulse laser. As described in Sec. I, there are two kinds of physical mechanisms of dendritic flux avalanches: one mechanism is thermally driven and the other is dynamically driven. In the former, the avalanches are activated by a slow ramping of applied magnetic field, i.e., gradually increasing forces of mutual repulsion and interaction in a vortex matter up to a critical value until the metastable state is broken. In the latter, the avalanches are activated by a local temperature variation. Once some vortices detach from their pinning sites and start to move in the superconductor, there is an accompanying dissipation of energy. This dissipation increases the local temperature in the superconductor and facilitates further motions of other vortices, which result in further heating of the superconductor. This positive feedback may sweep away the critical state and translate into a lightning flux avalanche in the superconductor [25]. However, once an avalanche is formed, it is difficult to determine its mechanism. Here, we perform two groups of experiments. In the first case, the laser spot is in the mixed state, and representative results are shown in Figs. 6(a)–6(d), which illustrate the evolution of the flux avalanche over time. Figures 6(e)–6(h) display the avalanche process at the same temperature and

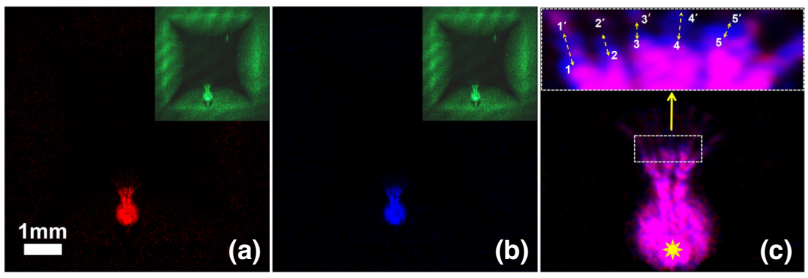

FIG. 5. (a),(b) Examples of double-exposure flux avalanche grayscale images under the same experimental conditions. The insets display the original MOI pictures. (c) Superposition of the two colors (red and blue) with the same exposure time of 8.37 ns; the inset displays five groups of position coordinates to calculate the Lyapunov exponent. The numbers 1, 2, 3, 4, and 5 and 1', 2', 3', 4', and 5' indicate location of the avalanche in the second exposure time when induced by the first and second laser pulses, respectively.

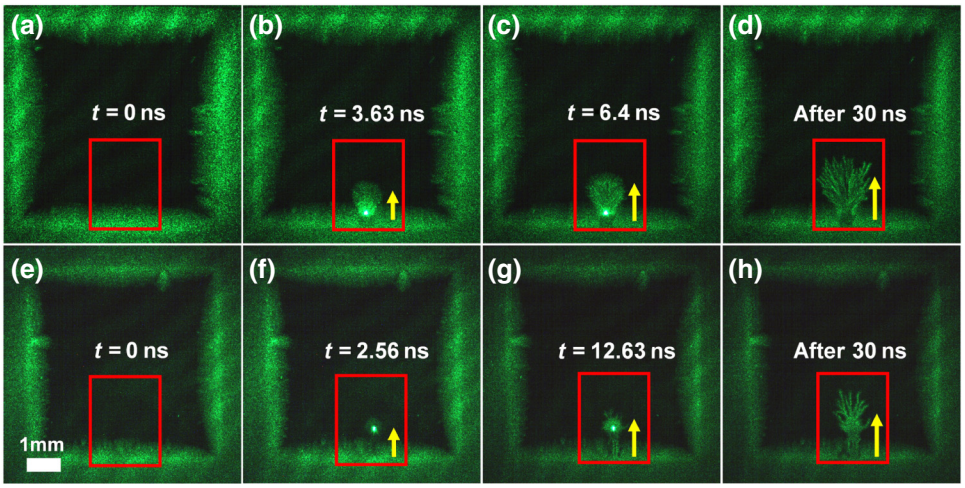

FIG. 6. (a)–(d) Representative results of flux avalanche patterns with time triggered by a pulse laser, where the laser spot is located in the mixed state. (e)–(h) Similar results under the same experimental conditions, except the laser spot is located in the Meissner region. White bright spot denotes the position of the laser spot, and yellow arrows indicate the direction of the flux avalanche.

magnetic field, except the laser spot is in the Meissner state. The ordinary view of the development of laser-triggered avalanches is that the avalanche root should be located at the laser spot because that is where the vortices are motivated. However, the experimental results do not support this view. From Fig. 6, the rule of avalanche evolution is concluded to be as follows: the pulse laser heats the superconducting material and increases the local temperature, which reduces local flux pinning. The decrease in the pinning force, f_p, will destroy the metastable equilibrium state, that is, $f_p < f_L$, in which f_L denotes that the driving-force (magnetic pressure) action on a vortex has a Lorentz-like form, $\vec{f_L} = \vec{J} \times \Phi_0 \vec{z}$, where $\vec{J}$ is the local density of a magnetization current and Φ_0 is a flux quantum. Thus, some vortices (around laser spot) become detached from pinning centers and start to enter into the Meissner state along the direction of the magnetic pressure, which can be verified by the dark trail behind the moving vortices. With evolution of the avalanche, an increasing number of vortices are pushed in and form the dendritic flux avalanche. As a result, the root of the avalanche is located at the edge of the superconducting film, regardless of whether the laser position is in the mixed state or the Meissner state. Laser-triggered avalanches are driven by electromagnetic forces, which is well demonstrated. For the present avalanche triggered by a pulse laser, we also think it is worth discussing our results with respect to the SOC. Figure S3 (Sec. D) within the Supplemental Material [38] displays a statistical analysis, where the avalanche size is taken as the number of avalanche bifurcations. One can see from the two figures that there is a good linear relationship between the logarithmic coordinates of branched bifurcations and the bifurcation frequency. The red straight lines, with slopes of -1.17 and -1.63, are provided as a guide to the eye. Our measured avalanche exponents are close to those obtained from experimental [25,26,42] and numerical simulations [43].

IV. CONCLUSION

We investigate the behavior of dendritic flux avalanches triggered by a pulse laser. We study the SDIC of the laser-triggered flux avalanches based on multiexposure technology within the classical MOI framework, and we find a series of positive Lyapunov exponents between two simultaneous trajectories, which can be considered direct evidence for the chaotic dynamics of the avalanche. Notably, we can determine that the physical mechanism of the present avalanche is driven by electromagnetic forces, given that the root of the present avalanche is located at the edge of the superconducting material. In the end, we also find the avalanche triggered by a laser shows the SOC, which is similar to traditional thermomagnetic instability.

ACKNOWLEDGMENTS

This work is supported by the Fund of Natural Science Foundation of China (Grants No. 11872196 and No. 11902130). This work is also supported by the Fundamental Research Funds for the Central Universities (Grant No. lzujbky-2018-9) and 111 Project (B14044).

[1] E. Altshuler, T. H. Johansen, Y. Paltiel, P. Jin, K. E. Bassler, O. Ramos, Q. Y. Chen, G. F. Reiter, E. Zeldov, and C. W. Chu, Vortex avalanches with robust statistics observed in superconducting niobium, Phys. Rev. B. **70**, 140505 (2004).

[2] C. A. Duran, P. L. Gammel, R. E. Miller, and D. J. Bishop, Observation of magnetic-field penetration via dendritic growth in superconducting niobium films, Phys. Rev. B. **52**, 75 (1995).

[3] I. A. Rudnev, D. V. Shantsev, T. H. Johansen, and A. E. Primenko, Avalanche-driven fractal flux distributions in NbN superconducting films, Appl. Phys. Lett. **87**, 042502 (2005).

[4] E. Baruch-El, M. Baziljevich, T. H. Johansen, X. Y. Zhou, X. Q. Jia, B. B. Jin, A. Shaulov, and Y. Yeshurun, Magnetic

flux instability in NbN films exposed to fast field sweep rates, Supercon, Sci. Technol. **31**, 105008 (2018).
[5] P. Mikheenko, T. H. Johansen, S. Chaudhuri, I. J. Maasilta, and Y. M. Galperin, Ray optics behavior of flux avalanche propagation in superconducting films, Phys. Rev. B. **91**, 060507 (2015).
[6] S. Treiber, C. Stahl, G. Schütz, and J. Albrecht, Unusual flux jumps above 12K in non-homogeneous MgB2 thin films, Supercond. Sci. Technol. **25**, 065010 (2012).
[7] F. L. Barkov, D. V. Shantsev, T. H. Johansen, P. E. Goa, W. N. Kang, H. J. Kim, E. M. Choi, and S. I. Lee, Local threshold field for dendritic instability in superconducting MgB2 films, Phys. Rev. B. **67**, 064513 (2003).
[8] J. Albrecht, A. T. Matveev, J. Strempfer, H. U. Habermeier, D. V. Shantsev, Y. M. Galperin, and T. H. Johansen, Dramatic Role of Critical Current Anisotropy on Flux Avalanches in MgB2 Films, Phys. Rev. Lett. **98**, 117001 (2007).
[9] E. Baruch-El, M. Baziljevich, B. Y. Shapiro, T. H. Johansen, A. Shaulov, and Y. Yeshurun, Dendritic flux instabilities in $YBa_2Cu_3O_{7-x}$ films: Effects of temperature and magnetic field ramp rate, Phys. Rev. B. **94**, 054509 (2016).
[10] E. Baruch-El, M. Baziljevich, T. H. Johansen, and Y. Yeshurun, Substrate influence on dendritic flux instability in YBCO thin films, J. Supercond. Novel Magn. **28**, 379 (2014).
[11] M. Baziljevich, E. Baruch-El, T. H. Johansen, and Y. Yeshurun, Dendritic instability in $YBa_2Cu_3O_{7-\delta}$ films triggered by transient magnetic fields, Appl. Phys. Lett. **105**, 012602 (2014).
[12] U. Bolz, D. Schmidt, B. Biehler, B. U. Runge, R. G. Mints, K. Numssen, H. Kinder, and P. Leiderer, Dendritic and homogeneous regimes of flux penetration into YBCO films, Physica C. **388-389**, 715 (2003).
[13] V. Bujok, P. Brüll, J. Boneberg, S. Herminghaus, and P. Leiderer, Nanosecond magneto-optic study of a new instability in thin $YBa_2Cu_3O_{7-\delta}$ films, Appl. Phys. Lett. **63**, 412 (1993).
[14] P. Leiderer, J. Boneberg, P. Brull, V. V. Bujok, and S. Herminghaus, Nucleation and Growth of a Flux Instability in Superconducting $YBa_2Cu_3O_{7-\delta}$ Films, Phys. Rev. Lett. **71**, 2646 (1993).
[15] U. Bolz, B. Biehler, D. Schmidt, B. U. Runge, and P. Leiderer, Dynamics of the dendritic flux instability in $YBa_2Cu_3O_{7-\delta}$ films, Europhys. Lett. **64**, 517 (2003).
[16] A. Lara, F. G. Aliev, V. V. Moshchalkov, and Y. M. Galperin, Thermally Driven Inhibition of Superconducting Vortex Avalanches, Phys. Rev. Appl. **8**, 034027 (2017).
[17] A. Lara, F. G. Aliev, A. V. Silhanek, and V. V. Moshchalkov, Microwave-stimulated superconductivity due to presence of vortices, Sci. Rep. **5**, 9187 (2015).
[18] G. Ghigo, F. Laviano, L. Gozzelino, R. Gerbaldo, E. Mezzetti, E. Monticone, and C. Portesi, Evidence of rf-driven dendritic vortex avalanches in MgB2 microwave resonators, J. Appl. Phys. **102**, 113901 (2007).
[19] Z. Jing, H. Yong, and Y. Zhou, Numerical simulation on the flux avalanche behaviors of microstructured superconducting thin films, J. Appl. Phys. **121**, 023902 (2017).
[20] J. I. Vestgarden, D. V. Shantsev, Y. M. Galperin, and T. H. Johansen, Lightning in superconductors, Sci. Rep. **2**, 886 (2012).
[21] J. I. Vestgården, F. Colauto, A. M. H. de Andrade, A. A. M. Oliveira, W. A. Ortiz, and T. H. Johansen, Cascade dynamics of thermomagnetic avalanches in superconducting films with holes, Phys. Rev. B. **92**, 144510 (2015).
[22] J. I. Vestgården, Y. M. Galperin, and T. H. Johansen, Oscillatory regimes of the thermomagnetic instability in superconducting films, Phys. Rev. B. **93**, 174511 (2016).
[23] T. Qureishy, J. I. Vestgården, A. J. Qviller, A. S. Fjellvåg, J. M. Meckbach, A. Torgovkin, T. H. Johansen, K. Ilin, M. Siegel, I. Maasilta, and P. Mikheenko, Energy of dendritic avalanches in thin-film superconductors, AIP Advances. **8**, 085128 (2018).
[24] J. I. Vestgarden, T. H. Johansen, and Y. M. Galperin, Nucleation and propagation of thermomagnetic avalanches in thin-film superconductors, Low Temp. Phys. **44**, 603 (2018).
[25] E. Altshuler and T. H. Johansen, Colloquium: Experiments in vortex avalanches, Rev. Mod. Phys. **76**, 471 (2004).
[26] A. J. Qviller, V. V. Yurchenko, Y. M. Galperin, J. I. Vestgården, P. B. Mozhaev, J. B. Hansen, and T. H. Johansen, Quasi-One-Dimensional Intermittent Flux Behavior in Superconducting Films, Phys. Rev. X. **2**, 011007 (2012).
[27] B. Eckhardt, Quantum-mechanics of classically non-integrable systems, Phys. Rep. **163**, 205 (1988).
[28] M. Toda, S. Adachi, and K. Ikeda, Dynamical aspects of quantum-classical correspondence in quantum chaos, Prog. Theor. Phys. Supp. **98**, 323 (1989).
[29] A. A. Abrikosov, On the magnetic properties of superconductors of the second group, Sov. Phys. JETP. **5**, 1174 (1957).
[30] R. V. Jensen, Quantum chaos, Nature **355**, 311 (1992).
[31] E. Olive and J. C. Soret, Chaos and plasticity in superconductor vortices: Low-dimensional dynamics, Phys. Rev. B. **77**, 144514 (2008).
[32] M. Lu-Dac and V. V. Kabanov, Phase Slip Phenomena in Superconductors: From Ordered to Chaotic Dynamics, Phys. Rev. Lett. **105**, 157005 (2010).
[33] T. Bohr, P. Bak, and M. H. Jensen, Transition to chaos by interaction of resonances in dissipative systems. II. Josephson-junctions, charge-density waves, and standard maps, Phys. Rev. A. **30**, 1970 (1984).
[34] A. E. Botha, I. R. Rahmonov, and Y. M. Shukrinov, Spontaneous and controlled chaos synchronization in intrinsic josephson junctions, IEEE Trans. Appl. Supercond. **28**, 1800806 (2018).
[35] J. Levy, M. S. Sherwin, and J. Theiler, Time-Domain Study of Low-Dimensional Chaos in the Switching Charge-Density-Wave Conductor NbSe3, Phys. Rev. Lett. **70**, 2597 (1993).
[36] A. Zettl, M. S. Sherwin, and R. P. Hall, Dynamics of charge-density wave conductors - broken coherence, chaos, and noisy precursors, Physica B & C. **143**, 69 (1986).
[37] A. A. Chernikov and G. Schmidt, Adiabatic chaos in Josephson-junction arrays, Phys. Rev. E. **50**, 3436 (1994).
[38] See the Supplemental Material http://link.aps.org/supplemental/10.1103/PhysRevApplied.13.024036 for calculating the critical current of YBCO films via the MOI technology

in Sec. A, which includes Refs. [44,45]. In Sec. D, a brief study of the SOC can be found, which includes Refs. [1,26].

[39] A. Wolf, J. B. Swift, H. L. Swinney, and J. A. Vastano, Determining lyapunov exponents from a time-series, Physica D. **16**, 285 (1985).

[40] X. Zeng, R. Eykholt, and R. A. Pielke, Estimating the Lyapunov-Exponent Spectrum From Short-Time Series of low Precision, Phys. Rev. Lett. **66**, 3229 (1991).

[41] B. Eckhardt, G. Hose, and E. Pollak, Quantum-mechanics of a classically chaotic system - observations on scars, periodic-orbits, and vibrational adiabaticity, Phys. Rev. A. **39**, 3776 (1989).

[42] C. M. Aegerter, M. S. Welling, and R. J. Wijngaarden, Self-organized criticality in the bean state in YBa2Cu3O7-x thin films, Europhys. Lett. **65**, 753 (2004).

[43] R. Mulet, R. Cruz, and E. Altshuler, Thermally activated avalanches in type-II superconductors, Phys. Rev. B. **63**, 094501 (2001).

[44] C. Liu, X. Zhang, and Y.-H. Zhou, A novel design for magneto-optical microscopy and its calibration, Meas. Sci. Tech. **30**, 115904 (2019).

[45] F. Laviano, D. Botta, A. Chiodoni, R. Gerbaldo, G. Ghigo, L. Gozzelino, S. Zannella, and E. Mezzetti, An improved method for quantitative magneto-optical analysis of superconductors, Supercond. Sci. Tech. **16**, 71 (2003).